Journal of Medicinal Chemistry

Brief Article

New Insights into Human 17#-Hydroxysteroid Dehydrogenase Type 14: First Crystal Structures in Complex with a Steroidal Ligand and with a Potent Non-Steroidal Inhibitor

Nicole Bertoletti, Florian Braun, Mahalia Lepage, Gabriele Möller, Jerzy Adamski, Andreas Heine, Gerhard Klebe, and Sandrine Marchais-Oberwinkler

J. Med. Chem., **Just Accepted Manuscript** • DOI: 10.1021/acs.jmedchem.6b00293 • Publication Date (Web): 30 Jun 2016

ACS Publications

Journal of Medicinal Chemistry is published by the American Chemical Society. 1155 Sixteenth Street N.W., Washington, DC 20036

New Insights into Human 17β-Hydroxysteroid Dehydrogenase Type 14: First Crystal Structures in Complex with a Steroidal Ligand and with a Potent Non-Steroidal Inhibitor

Nicole Bertoletti[†¥], Florian Braun[†¥], Mahalia Lepage[†], Gabriele Möller[‡], Jerzy Adamski[‡§$], Andreas Heine[†], Gerhard Klebe[†], Sandrine Marchais-Oberwinkler.[†*]

[†] Philipps University Marburg, Institute for Pharmaceutical Chemistry, 35037 Marburg, Germany

[‡]Helmholtz Zentrum München, German Research Center for Environmental Health, Institute of Experimental Genetics, Genome Analysis Center, 85764 Neuherberg, Germany

[§] Lehrstuhl für Experimentelle Genetik, Technische Universität München, 85350 Freising-Weihenstephan, Germany

[$] German Center for Diabetes Research (DZD), 85764 Neuherberg, Germany

KEYWORDS. 17β-HSD14, crystal structures, first potent inhibitor, steroidal and non-steroidal ligand, thermal shift assay.

ABSTRACT: 17β-HSD14 is a SDR enzyme, able to oxidize estradiol and 5-androstenediol using NAD^+. We determined the crystal structure of this human enzyme as the holo form and as ternary complexes with estrone and with the first potent, non-steroidal inhibitor. The structures reveal a conical, rather large and lipophilic binding site and are the starting point for structure-based inhibitor design. The two natural variants (S205 and T205) were characterized and adopt a similar structure.

INTRODUCTION

17β-Hydroxysteroid dehydrogenase type 14 (17β-HSD14),[1,2] also called retSDR3, DHRS10 or SDR47C19, is the latest 17β-HSD which has been identified. It belongs to the SDR (Short-chain Dehydrogenase-Reductase) family. Its physiological role is yet unknown. Estradiol (E2), 5-androstene-3β,17β-diol (5-diol) and testosterone (T) have been identified as substrates *in vitro*.[2] 17β-HSD14 catalyzes the alcohol oxidation of the aforementioned estrogens and androgens at their position 17 giving rise to estrone (E1), dehydroepiandrosterone (DHEA), and 4-androstene-3,17-dione (4-dione), respectively.[2] The enzyme requires NAD^+ as cofactor.

17β-HSD14 is a cytosolic enzyme.[2] Concerning its localization, northern blot analyses have shown that the human HSD17B14 gene is dominantly expressed in the brain, liver, placenta,[2] and in the kidney.[3] In another study, using immunochemical based methods Sivik *et al.*[4] demonstrated that the protein is also expressed in adrenals and testis as well as in eye, heart, kidney, esophagus, liver, rectum, salivary glands and skeletal muscle. 17β-HSD14 has also been identified in breast cancer tissue.[5]

The gene coding for 17β-HSD14 was first isolated from the human retinal epithelium by Haeseleer[3] and contains a serine at position 205 (S205). An alternate version of the gene was subsequently isolated from a melanotic melanoma cell during a genome sequencing campaign.[6] This allelic variant, termed T205, carries a threonine at position 205. The meaning of the observed polymorphism has not been analyzed until now and the T205 variant has also never been characterized to date. In this study, the structural and the biochemical characterization of the T205 will be addressed as well as its comparison to the S205 enzyme.

The S205 variant of *h*17β-HSD14 has been crystallized and the 3D-structure of the apoenzyme determined by Lukacik *et al.*[2] Crystal structures of a target protein provide important structural insights into binding sites. However from the existing structure no information about the protein/ligand interaction, either with the cofactor or with the substrate, can be extracted.

Furthermore, inhibitors are important tools not only to characterize the binding site of a protein but also to study the physiological role of a protein *in vivo*. No inhibitor of this enzyme has been reported to date. In the following, the first potent non-steroidal inhibitor of *h*17β-HSD14 is described. The ternary complex enzyme-cofactor-inhibitor was also crystallized and its structure determined.

In the present study the description of the new variant T205 as well as five new crystal structures provide further insights in the characterization of this enzyme.

RESULTS AND DISCUSSION

Identification of the first *h*17β-HSD14 inhibitor. The dihydroxyphenylpyridine methanone compound class **1**, previously described as weak *h*17β-HSD2 inhibitors,[7] was chosen as the initial scaffold. Several modifications, to be described in detail elsewhere, were accomplished to feature compound **2** (Figure 1). This compound is the first reported *h*17β-HSD14 inhibitor (see Supporting Information SI). As measured in a fluorimetric assay, it shows a K_i= 7±1 nM.

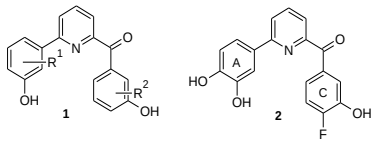

Figure 1. Structure of dihydroxyphenylpyridine methanone scaffold **1** and compound **2**.

Protein expression and purification. Both recombinant *h*17β-HSD14 protein variants (S205 and T205) were overexpressed in *E.coli* BL21 pLysS via transformation with the corresponding *N*-6His-tag plasmid, following Lukacik's procedure,[2] applying minor modifications (see SI). Pure enzyme was obtained with a yield between 8 - 15 mg of protein per liter of bacterial culture. The specific activity was 1.35 and 1.21 nmol.min^{-1}.mg^{-1} for S205 and T205, respectively, in presence of E2.

Protein stability and Thermal Shift Assay (TSA) experiment. The main challenge encountered during the protein purification was the low stability of *h*17β-HSD14.

Table 1. Effect of different buffer additives on the T_m of *h*17β-HSD14

	T_{m1} in °C	T_{m2} in °C
No additive	35.5	59.0
Glycerol 20%		57.5
MPD 10%		47.0
PEG400 10%		53.0
Ethylene glycol 10%		53.0
Glucose 250 mM	37.5	59.5
NAD$^+$ 0.2 mM	41.5	59.0
Glucose 250 mM, NAD$^+$ 0.25 mM	48.5	59.0

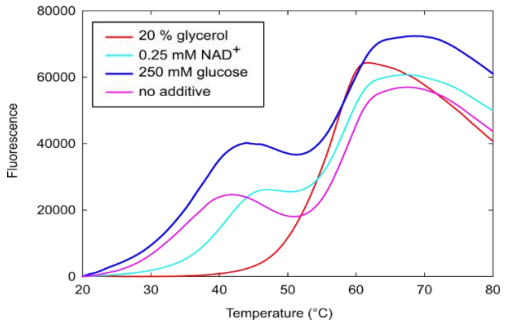

Figure 2. TSA curves of *h*17β-HSD14 obtained in presence of glycerol (red), NAD$^+$ (cyan), glucose (blue) or without any additive (magenta).

In the absence of any buffer additives, no or only minor amounts of protein could be isolated. Glycerol is known to stabilize proteins by compacting their structures to a globular shape[8] and its addition substantially increased the efficiency of protein purification. However, it must be emphasized that glycerol in presence of NAD$^+$ and the enzyme, without substrate, induces the production of a fluorescent substance which, after investigation, turned out to have the same fluorescence fingerprint as NADH. We concluded that glycerol is recognized as a substrate by *h*17β-HSD14, thereby transforming NAD$^+$ into NADH. Ethylene glycol, MPD and PEG400 caused the same effect as observed with glycerol. Glucose, which is commonly used as a cryo protectant and is also known to stabilize proteins,[9] was identified not to be a substrate and was therefore added during purification. The protein was further stabilized by adding NAD$^+$ (0.5 mM) during the purification steps and for storage (0.25 mM).

Glycerol is often used as protein stabilizer during activity assays. To the extent of our knowledge, it is not systematically investigated whether or not glycerol can be accepted as a substrate during enzymatic assays, and whether it interferes with substrate binding. The presence of glycerol might therefore lead to some discrepancies in the interpretation of biological results.

The search for sufficient stabilization conditions, compatible with our fluorimetric activity assay, was supported by TSA, which validates the amount of stabilization of a protein upon addition of different buffer additives (Figure 2). The reference curve was obtained in the absence of any additive and revealed two inflection points (T_{m1}= 35.5 °C, T_{m2}= 59 °C, Table 1). Conversely, in the presence of glycerol, a curve with one single melting point can be observed (T_m= 57.5 °C), indicating that it effectively stabilizes the protein. Similar curves were obtained with MPD, PEG400 and ethylene glycol, but at lower melting temperatures than observed with glycerol (Table 1). This indicates a weaker stabilizing effect on the protein.

Remarkably, adding glucose or NAD$^+$ resulted in TSA curves with two maxima. Both molecules independently induced a slight shift in the T_{m1} of the protein but did not greatly affect the T_{m2}. The combination of glucose and NAD$^+$ has a greater influence on T_{m1} (ΔT_{m1}= +13°C, compared to the measurement without any additive) while T_{m2} remains unchanged. This result suggests that the first maximum corresponding to T_{m1} might represent a fraction of the protein in a less-stable conformation, while the second maximum T_{m2} represents the true melting point of the protein in its most stable conformation.

The influence of different ligands on *h*17β-HSD14 stabil-

Table 2. Effect of different ligands on the T_m of *h*17β-HSD14

	T_m in °C
DMSO 2.5%	56.0
Estradiol 0.25 mM	58.0
Estrone 0.25 mM	57.5
Compound **2** 0.25 mM	70.5

ity was also tested. Pure DMSO was used as control and a T_m of 56°C was obtained (Table 2). No second maximum was identified. In the presence of E1 and E2, only a slight shift could be observed (ΔT_m= 1.5-2°C). However, the strongest positive shift was recorded upon addition of our inhibitor (ΔT_m= 14.5°C), indicating that compound **2** has a strong affinity for the protein resulting in a strong stabilizing effect.[10,11]

Activity assay and biochemical characterization of both S205 and T205. The activity of *h*17β-HSD14 was determined by fluorimetric intensity measurement of NADH formed during the catalytic reaction. The reaction was carried out using the purified enzyme, E2 as substrate and NAD^+ as cofactor (see SI). High substrate concentration (32 µM) had to be applied because of the low sensitivity of the method. All the other 17β-HSDs have the characteristic ability to perform both oxidative and reductive reactions *in vitro* depending on the oxido-reduction state of the cofactor. Therefore, the activity of *h*17β-HSD14 in the presence of E1 and NADH (corresponding to the back reaction) was also tested. However, no conversion to NAD^+ could be detected after 15 min. *In vivo*, the cytoplasmic NAD^+ concentration is about 500 times higher than NADH. This indicates that *in vivo* this enzyme should be a pure dehydrogenase. In order to carry out a biochemical comparison of S205 and T205 variants, kinetic experiments were performed with the substrates E2, 5-diol and T. With all substrates, the enzyme follows Michaelis-Menten kinetics. However, with testosterone, no saturation curve could be observed, and consequently the kinetic parameters could not be determined. For 5-diol and E2 the Michaelis-Menten constants (K_m), the maximum velocities (V_{max}) and the turnover rate values (k_{cat}) were determined (Table 3). For the S205 variant, the Km values obtained are in the same range as those published by Lukacik *et al.*[2] The kinetic data of the T205 variant are very similar to those of the S205 protein, indicating that the T205 mutation does not influence the catalytic efficiency of the enzyme. This result appears reasonable as the amino acid 205 is not close to the catalytic triad. The rather high Km and low turnover of *h*17β-HSD14 for both, 5-diol and E2, had already been pointed out by Lukacik *et al.*[2] and might indicate that the enzyme could bind other types of substrates.

Crystallization of *h*17βHSD14. Our crystallization trials led to five different crystal structures: *h*17β-HSD14 as apoenzyme (S205), as binary complexes with NAD^+ (with both variants S205 and T205), as a complex with the product E1 (T205) and as a complex with the first non-steroidal inhibitor **2** (T205). All crystal structures were obtained by co-crystallization (see SI). The data processing and the refinement statistics are summarized in Table 4.

The apo structure was reproduced using different crystallization conditions than those described by Lukacik *et al.*,[2] leading to a structure of 1.52 Å resolution. In the apo form a homotetramer is present in the asymmetric unit of the monoclinic space group $P12_11$ (Figure 3A). It exhibits the A2B2 symmetry as described by Lukacik *et al.*,[2] however, in this new structure the C-terminus segment is visible. The tetramer is built-up by the interaction of two identical dimers (A2 and B2) each composed of two monomers. The two dimers A2 and B2 differ in the conformation of the flexible loop, formed by the α-helices αFG1 and αFG2 (residues 189–212), which is open in A2 and closed in B2. A maximum shift of about 7 Å is observed between the two conformations of the flexible loop, which adjusts the size of the active site (Figure 3B). In the dimer A2, the C-terminus of each monomer is inserted into the wide-open active site of the opposite monomer.

In the case of the holo structure, both variants of the protein S205 and T205 were co-crystallized in complex with NAD^+. Both variants contain only one monomer in the asymmetric unit in the cubic space group I23. Here, the tetramer is formed by four identical molecules. The PISA calculation[12] with a total buried area of 6610 Å² for each monomer and the analysis by native ESI mass spectrometry (result not shown) support that the tetrameric form is the assembly present in solution. No structural differences between the S205 and the T205 holoenzymes were evident from their 3D-structures as both isoforms were identical, with the mutated amino acid being the only exception (Figure 3C). The flexible loop (αFG1 and αFG2) is fixed in a closed conformation, which reduces the volume of the binding pocket. The active site cleft is also downsized by the presence of Tyr253 belonging to the C-terminus from the adjacent crystal mate. The C-terminal part of the monomer is completely defined in the density and reveals a different conformation compared to the dimer A2 of the apo structure: it is not entering the binding pocket of the monomer but it is arranged around the surface of the bordering monomer (Figure S8). No further major conformational changes are observed.

In the structure of both ternary complexes, the monomers, present in the asymmetric unit, interact with each other similarly to the holo form, generating a tetramer via crystal symmetry. The C-terminal tails of the complex with E1 and with compound **2** are very flexible and the

Table 3. Kinetic analysis of *h*17β-HSD14 and enzymatic specific activity.

	S205			T205		
Substrate	K_m (µM)	V_{max} (nM.min^{-1})	k_{cat} (min^{-1})	K_m (µM)	V_{max} (nM.min^{-1})	k_{cat} (min^{-1})
5-diol	6.6±1.5	58±0.4	0.017	7.8±1.2	68±0.3	0.019
E2	6.2±1.4	82±0.1	0.024	7.9±1.7	114±0.3	0.033

Mean values and given standard deviations were calculated based on 5 - 7 measurements.

amino acids from Ser258 to Ile268 are not defined by the electron density map. Only Pro269, Ser270 and Gly271, which are stabilized by a contact with the asymmetrical equivalent molecule, can be seen. A backbone comparison between the holo form and the ternary complexes does not reveal any differences between the structures. Both, E1 and the inhibitor, are located in the steroid binding pocket. The substrate binding site has a conical shape, with the catalytic triad being at the apex of the cone and a wide solvent-exposed opening at the other side.

In all the structures the catalytic triad, composed of Ser141, Tyr154 and Lys158, maintains an identical geometry. A special attention should be paid to His93, which is stabilized by Gln148, located in the substrate binding site and close to the catalytic triad because it is not present in other human SDR 17β-HSDs. This fact might be exploited to optimize the inhibitor structures in order to achieve specific interactions with *h*17β-HSD14 and thereby in-

Table 4. Data collection and refinement statistic for the crystal structures.

PDB ID code [a]	Apo structure 5ICS	Holo structure S205 5JSF	Holo structure T205 5JS6	E1 complex 5HS6	Inhibitor 2 complex 5ICM
(A) Data collection and processing					
space group	$P12_11$	$I23$	I23	$I422$	$I422$
unit cell parameters *a*, *b*, *c* (Å)	77.0, 92.2, 87.3	130.2, 130.2, 130.2	130.2, 130.2, 130.2	91.0, 91.0, 131.9	91.7, 91.7, 133.8
Matthews coefficient [b] (Å^3/Da)	2.5	3.2	3.22	2.4	2.4
solvent content [b] (%)	49.9	61.7	61.7	49.0	49.9
(B) Diffraction data					
resolution range (Å)	50-1.52 (1.61-1.52)	50-1.84 (1.95-1.84)	50-2.00 (2.12-2.00)	50-2.02 (2.14-2.02)	50-1.68 (1.78-1.68)
unique reflections	169468 (27103)	31827 (5106)	24734 (3933)	18613 (2930)	34525 (5122)
$R(I)_{sym}$ (%)	5.8 (48.1)	4.7 (49.1)	4.2 (48.3)	9.1 (48.6)	8.1 (49.3)
Wilson *B* factor (Å^2)	13.72	35.06	44.6	26.13	19.96
completeness (%)	99.5 (98.8)	99.9 (99.6)	99.4 (98.5)	99.7 (98.7)	99.1 (98.3)
redundancy	3.8 (3.8)	6.6 (6.8)	6.6 (6.5)	7.5 (7.6)	6.9 (6.7)
$<I/\sigma(I)>$	15.2 (2.7)	21.3 (4.2)	22.71 (3.91)	15.9 (4.3)	14.1 (2.9)
(C) Refinement					
resolution range (Å)	43.95-1.52	46.05-1.84	46.03-2.00	46.11-2.02	37.82-1.68
reflections used in refinement (work/free)	169468 (160994/8474)	31827 (30235/1592)	24734 (23497/1237)	18793 (17682/931)	32511 (30885/1626)
final *R* value for all reflections (work/free) (%)	0.13/0.16	0.16/0.19	0.17/0.19	0.16/0.19	0.16/0.19
protein residues	1033	268	268	257	255
water molecules	735	86	64	136	189
RMSD from ideality: bond lengths (Å)	0.008	0.007	0.007	0.007	0.009
RMSD from ideality: bond angles (°)	0.937	0.817	0.817	0.868	1.004
Ramachandran plot: [c]					
residues in most favored regions (%)	92.5	92.2	92.2	93.3	92.8
residues in additionally allowed regions (%)	7.5	7.8	7.8	6.7	7.2
residues in generously allowed regions (%)	0.0	0.0	0.0	0.0	0.0
residues in disallowed regions (%)	0.0	0.0	0.0	0.0	0.0
Mean *B* factor protein (Å^2) [d]	18.4	45.8	56.3	29.1	23.0
Mean *B* factor ligand (Å^2) [d]	-	-	-	44.9	26.1
Mean *B* factor water molecules (Å^2) [d]	32.2	49.7	56.0	35.6	32.9

[a] Values in parenthesis describe the highest resolution shell. [b] Calculated with Matthews_coef program from CCP4 suite version 6.4.0.[13] [c] Calculated with PROCHECK.[14] [d] Mean B factors were calculated with MOLEMAN.[15]

creasing selectivity toward other human SDR 17β-HSDs.

Description of the NAD$^+$, estrone, and inhibitor binding modes. Interactions stabilizing the cofactor in *h*17β-HSD14 are identified for the first time as the previously described structure did not contain NAD$^+$. The cofactor NAD$^+$ is buried inside the cofactor binding pocket and is coordinated via H-bond contacts to several amino acids and a number of crystallographically observed water molecules (Figure 4). These interactions are similar to those previously observed in other 17β-HSDs, for example in 17β-HSD10.[16]

E1, the product of the catalytic reaction, is found to be bound to the active site in an atypical fashion with its A-ring positioned in van der Waal's interaction distance to the nicotinamide portion of the cofactor (Figure 5A) thus placing the actual 17-reaction center in remote position relative to the cofactor. No apparent π-stacking interaction of the steroidal A-ring can be observed with any amino acid. The only H-bond interaction established is between the A-ring's hydroxyl group and the hydroxyl of Tyr154 of the catalytic triad (d= 2.5 Å). The carbonyl group in position 17 does not form any interactions, neither with any amino acid nor with the solvent. The steroidal C-ring is placed in the hydrophobic cleft formed by Trp192 and Leu95. The methyl group of the E1 is not detectable in the electron density of the ligand and therefore it was not included in the model. The orientation we do observe is, however, not unlikely due to the pseudo symmetry of E1,[17] and this also allows for the possibility that both orientations occur (with the 17 position of E1 binding to the catalytic triad or being away from it). No back reaction of the enzyme was observable by fluorescence assay. This result could be explained by the slow transformation rate of E1 to E2 or by the binding of E1 in a non-productive way or by both at the same time.

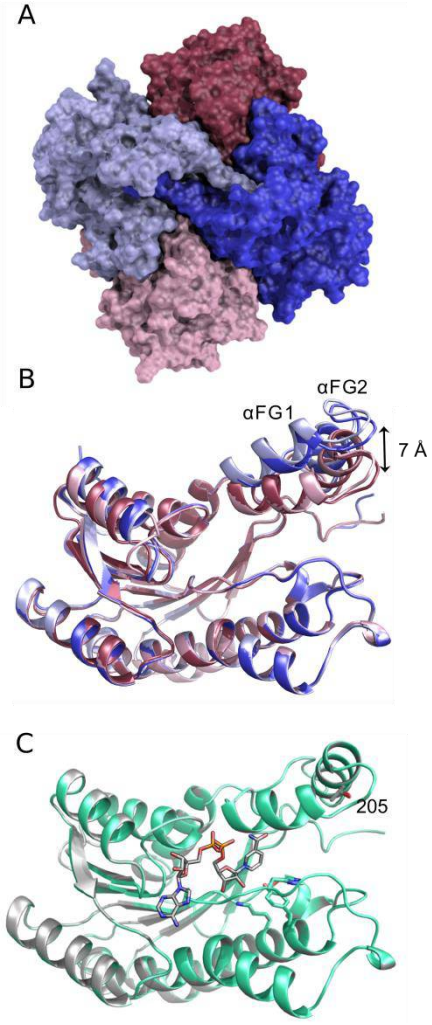

Figure 3. (A) Surface representation of the apoenzyme homotetramer (PDB code: 5ICS). (B) Ribbon representation of the superimposition of the four chains in the apo structure. The two chains forming dimer B2 are shown in pink shades and the two chains forming dimer A2 are shown in blue shades. (C) Ribbon representation of the superimposed binary complexes of variant S205 (greencyan) and T205 (gray) together with bound NAD$^+$; the catalytic triad and the residues 205 are shown as stick model (S205 PDB code: 5JSF, T205 PDB code: 5JS6). All structural representations were prepared with PvMOL.

Regarding compound **2**, the C-ring is located in vdW radius distance to the nicotinamide moiety of NAD$^+$ (Figure 5B). The hydroxyl group in position 3 of the C-ring establishes two hydrogen bonds to the OH groups of Ser141 (d= 2.6 Å) and Tyr154 (d= 2.4 Å), two amino acids being part of the catalytic triad. The two hydroxyl groups of the catechol A-ring form a polar interaction with the carbonyl backbone oxygen of Ala149 (d= 2.8 Å and d= 3.14 Å). Interestingly, the keto group between the pyridine and the C-ring does not form any interactions but seems to be important for the inhibitor to adopt the correct geometry. From the surface representation (Figure 5C), it becomes apparent that the V-shape of the inhibitor nicely complements the shape of the active site.

CONCLUSION

In this work, we have elucidated the first crystal structures of *h*17β-HSD14 in complex with ligands. The structure of the binary complex with the cofactor NAD$^+$ differs from the apoenzyme with respect to the flexible loop (αFG1 and αFG2 segment) which adopts a unique closed

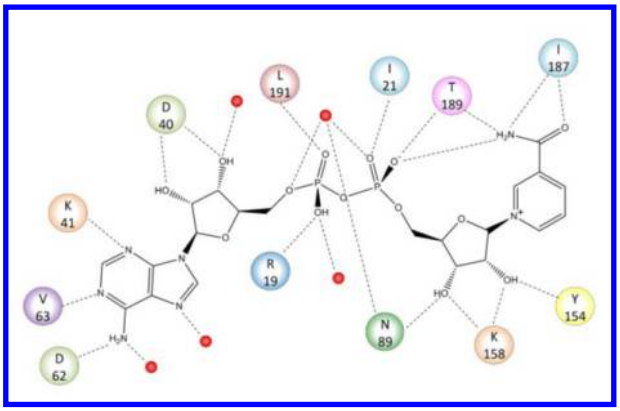

Figure 4. Interaction scheme between NAD$^+$ and *h*17β-HSD14 (PDB code: 5ICM). Water molecules are represented in red spheres. H-bond contacts are shown as dotted lines.

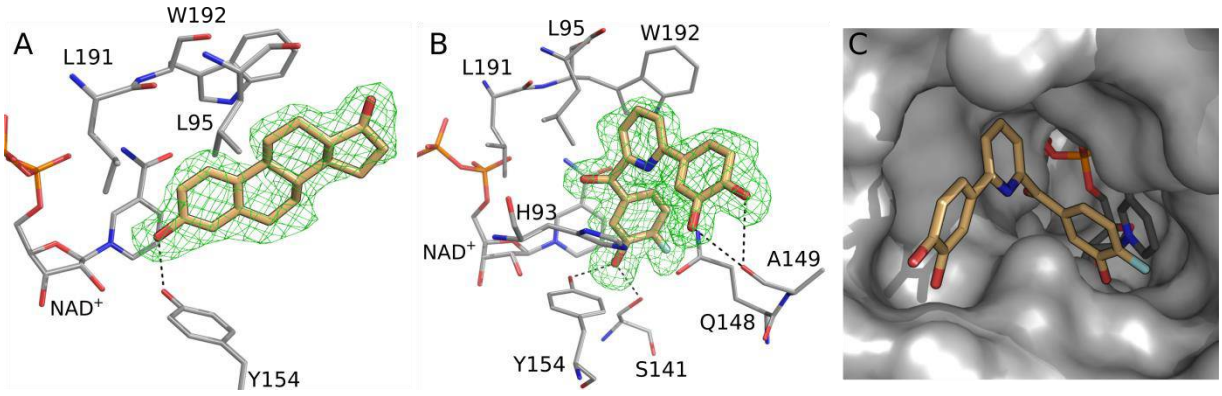

Figure 5. Crystal structures of *h*17β-HSD14 in complex with E1 (A, PDB code: 5HS6) and inhibitor **2** (B and C, PDB code: 5ICM). In panels A and B, estrone and inhibitor **2** are shown as stick model, the amino acids within a distance of 4.6 Å and cofactor are shown as thin lines. H-bond distances are depicted as dotted lines. *Fo-Fc* difference electron densities are shown as green mesh at a contour level of 2 σ. Panel C shows the protein as surface representation, cofactor and compound **2** as stick model.

conformation in the presence of NAD^+: it is found in either open (A2 dimer) or closed (B2 dimer) conformation without cofactor. The overall structure and the active site geometry in the ternary complexes with E1 or with compound **2** are very similar to those of the binary complex, with the flexible loop in the same closed state delimiting an elongated and conical active site. Binding of the cofactor appears to induce a shift of the flexible loop, which reduces the size of the active site and thereby produces the active conformation of the enzyme.

The ternary complex with inhibitor **2** is the most interesting structure obtained in this study as it describes the binding mode of the first non-steroidal *h*17β-HSD14 inhibitor in complex with the protein. It is striking that up to now no human SDR 17β-HSDs could ever be crystallized in complex with a non-steroidal compound. Several attempts have been conducted with 17β-HSD1 but all failed, possibly owing to the lipophilicity of the active site or the flexibility of the compounds.

Compound **2** is the first *h*17β-HSD14 inhibitor identified. It binds in a competitive manner occupying the substrate binding site. It has a strong affinity for the enzyme, indeed it is stabilized by three additional interactions and adapts very tightly to the active site geometry owing to its V-shape. The knowledge of its binding pose is of utmost importance as it is a starting point not only for structure-based drug design of *h*17β-HSD14 inhibitors, but also to endow inhibitors with the required selectivity toward other 17β-HSDs. The identification of the first *h*17β-HSD14 inhibitor is a valuable tool to further investigate the physiological role of this enzyme. However, further studies are still necessary to investigate the endogenous substrate and the functional role of the enzyme *in vivo*.

EXPERIMENTAL SECTION

Chemical methods. Column chromatography was performed on silica gel (0.04-0.063 mm, Macherey-Nagel). Mass spectrometry was performed on a Q-Trap 2000 (Applied Biosystems) equipped with an electrospray interface (ESI). ^{1}H and ^{13}C NMR spectra were measured on a JEOL ECX-400 spectrometer in acetone-*d6* at 400 MHz and 100 MHz, respectively. Chemical shifts are reported in δ (parts per million: ppm), using residual peaks for the deuterated solvents as internal standard: 2.05 ppm (^{1}H NMR), 29.8 ppm and 206.3 ppm (^{13}C NMR). Signals are described as t, dd, ddd, dt and m for triplet, doublet of doublet, doublet of doublet of doublet, doublet of triplet and multiplet, respectively. All coupling constants (*J*) are given in Hertz (Hz). Infrared spectroscopy was performed on a Bruker ALPHA FT-IR spectrometer as neat sample. The compound has 99.1% chemical purity as evaluated by HPLC on a Shimadzu® LC-20 system. A RP C18 NUCLEODUR® (125 mm x 4 mm, 5 µm) column (Macherey-Nagel) was used as stationary phase. All solvents were HPLC grade. In a gradient run the percentage of acetonitrile in water was increased from initial concentration of 30% at 0 min to 90% at 15 min and kept at 90% for 5 min. UV spectra were recorded at a wavelength of 254 nm.

[6-(3,4-Dihydroxyphenyl)pyridin-2-yl]-(4-fluoro-3-hydroxyphenyl)-methanone (2).

$C_{18}H_{12}FNO_4$; MW: 325; mp: 180-181 °C; ^{1}H NMR: δ 8.07-8.00 (m, 2H), 7.87 (dd, *J* = 8.7 Hz, 2.0 Hz, ^{1}H), 7.83 (dd, *J* = 6.8 Hz, 1.5 Hz, 1H), 7.74 (ddd, *J* = 8.5 Hz, 4.5 Hz, 2.0 Hz, 1H),7.69 (d, *J* = 2.1 Hz, 1H), 7.53 (dd, *J* = 8.3 Hz, 2.1 Hz, 1H), 7.29 (t, *J* = 9.6 Hz, 1H), 6.93 (d, *J* = 8.3 Hz, 1H); ^{13}C NMR: δ 192.4, 156.6, 155.6, 155.4 (d, *J* = 249.4 Hz), 147.8, 146.3, 145.5 (d, *J* = 13.0 Hz), 139.0, 134.2, (d, *J* = 3.3 Hz), 131.3, 124.8 (d, *J* = 7.6 Hz), 122.4, 121.3 (d, *J* = 4.2 Hz), 119.8, 116.6 (d, *J* = 19.1 Hz), 116.3, 114.8; IR: 3388, 1661, 1599, 1583, 1526, 1235, 755 cm^{-1}; MS (ESI): 326 $(M+H)^+$.

ASSOCIATED CONTENT

Supporting Information.

Experimental sections. Determination details of the C-terminal tails for the dimer A2 of the apoenzyme crystal structure. Color coded surface representation of the binding pocket of *h*17β-HSD14 in complex with the inhibitor **2**. Stereo representations of Figure 5. Kinetic graphs. Molecular formula strings. Synthetic pathway and compounds characterization.

Accession code:

Atomic coordinates and experimental data for the crystal structure of apoenzyme (PDB ID: 5ICS), of holoenzyme (PDB ID: 5JSF and 5JS6), for the co-crystal structure of E1 (PDB ID: 5HS6) and of **2** (PDB ID: 5ICM) with *h*17β-HSD14 will be release upon article publication.

AUTHOR INFORMATION

Corresponding Author

*Phone: +49 6421 28 22880. E-mail: marchais@staff.uni-marburg.de

Author Contributions

The manuscript was written through contributions of all authors. All authors have given approval to the final version of the manuscript. ¥N.B. and F.B. contributed equally.

Notes

The authors declare no competing financial interest.

ACKNOWLEDGMENT

We thank Prof. U. Oppermann for the gift of plasmid HSD17B14S205. The authors are grateful to the Deutsche Forschungsgemeinschaft (MA-5287/1-1 and KL-1204/15-1) for financial support and to the Deutscher Akademischer Austauschdienst for the grant of M.L. Part of the research leading to these results has received funding from BioStruct-X (grant agreement N°283570). We appreciate the help of U. Linne (Univ. of Marburg) in the mass spectrometry. We are also thankful to the beamline staff at Elettra Sincrotrone (Triestre), BESSY II (Helmholtz-Zentrum Berlin) and European Synchrotron Radiation Facility (ESRF, Grenoble) for providing support during data collection and for financial support and travel grant. The authors also thank L. Zara and T. Bayet for the help during their internships.

ABBREVIATIONS

17β-HSD14: 17β-hydroxysteroid dehydrogenase type 14; SDR: short-chain dehydrogenase reductase; NAD(H): nicotinamide adenine dinucleotide; E2: estradiol; 5-diol: 5-androstene-3β,17β-diol; T: testosterone; E1: estrone; DHEA: dehydroepiandrosterone; 4-dione: 4-androstene-3,17-dione; TSA: thermal shift assay; T_m: melting temperature; MPD: 2-methyl-2,4-pentanediol; PEG: polyethylene glycol; PDB: Protein Data Bank; vdW: van der Waals, SI: supporting information.

REFERENCES

(1) Lukacik, P.; Kavanagh, K. L.; Oppermann, U. Structure and Function of Human 17β-Hydroxysteroid Dehydrogenases. *Mol. Cell. Endocrinol.* **2006**, *248*, 61–71.

(2) Lukacik, P.; Keller, B.; Bunkoczi, G.; Kavanagh, K.; Hwa Lee, W.; Adamski, J.; Oppermann, U. Structural and Biochemical Characterization of Human Orphan DHRS10 Reveals a Novel Cytosolic Enzyme with Steroid Dehydrogenase Activity. *Biochem. J.* **2007**, *402*, 419–427.

(3) Haeseleer, F.; Palczewski, K. Short-Chain Dehydrogenases/reductases in Retina. *Methods Enzymol.* **2000**, *316*, 372–383.

(4) Sivik, T.; Vikingsson, S.; Gréen, H.; Jansson, A. Expression Patterns of 17β-Hydroxysteroid Dehydrogenase 14 in Human Tissues. *Horm. Metab. Res.* **2012**, *44*, 949–956.

(5) Sivik, T.; Gunnarsson, C.; Fornander, T.; Nordenskjöld, B.; Skoog, L.; Stål, O.; Jansson, A. 17β-Hydroxysteroid Dehydrogenase Type 14 Is a Predictive Marker for Tamoxifen Response in Oestrogen Receptor Positive Breast Cancer. *PLOS ONE* **2012**, *7*, e40568.

(6) Mammalian Gene Collection (MGC) Program Team. Generation and Initial Analysis of More than 15,000 Full-Length Human and Mouse cDNA Sequences. *Proc. Natl. Acad. Sci.* **2002**, *99*, 16899–16903.

(7) Wetzel, M.; Gargano, E. M.; Hinsberger, S.; Marchais-Oberwinkler, S.; Hartmann, R. W. Discovery of a New Class of Bicyclic Substituted Hydroxyphenylmethanones as 17β-Hydroxysteroid Dehydrogenase Type 2 (17β-HSD2) Inhibitors for the Treatment of Osteoporosis. *Eur. J. Med. Chem.* **2012**, *47*, 1–17.

(8) Gekko, K.; Timasheff, S. N. Mechanism of Protein Stabilization by Glycerol: Preferential Hydration in Glycerol-Water Mixtures. *Biochemistry* **1981**, *20*, 4667–4676.

(9) Bondos, S. E.; Bicknell, A. Detection and Prevention of Protein Aggregation Before, During, and after Purification. *Anal. Biochem.* **2003**, *316*, 223–231.

(10) Vedadi, M.; Niesen, F. H.; Allali-Hassani, A.; Fedorov, O. Y.; Finerty, P. J.; Wasney, G. A.; Yeung, R.; Arrowsmith, C.; Ball, L. J.; Berglund, H.; Hui, R.; Marsden, B. D.; Nordlund, P.; Sundstrom, M.; Weigelt, J.; Edwards, A. M. Chemical Screening Methods to Identify Ligands That Promote Protein Stability, Protein Crystallization, and Structure Determination. *Proc. Natl. Acad. Sci.* **2006**, *103*, 15835–15840.

(11) Matulis, D.; Kranz, J. K.; Salemme, F. R.; Todd, M. J. Thermodynamic Stability of Carbonic Anhydrase: Measurements of Binding Affinity and Stoichiometry Using ThermoFluor. *Biochemistry* **2005**, *44*, 5258–5266.

(12) Krissinel, E.; Henrick, K. Inference of Macromolecular Assemblies from Crystalline State. *J. Mol. Biol.* **2007**, *372*, 774–797.

(13) Collaborative Computational Project, Number 4. The CCP4 Suite: Programs for Protein Crystallography. *Acta Crystallogr. sect. D: Biol. Crystallogr.* **1994**, *50*, 760–763.

(14) Laskowski, R. A.; MacArthur, M. W.; Moss, D. S.; Thornton, J. M. PROCHECK: A Program to Check the Stereochemical Quality of Protein Structures. *J. Appl. Crystallogr.* **1993**, *26*, 283–291.

(15) Kleywegt, G. J.; Zou, J.-Y.; Kjeldgaard, M.; Jones, T. A. Around O. In *International Tables for Crystallography Volume F: Crystallography of biological macromolecules;* Rossmann, M. G., Arnold, E., Eds.; Springer Netherlands: Dordrecht, **2001**; pp 353–356.

(16) Powell, A. J.; Read, J. A.; Banfield, M. J.; Gunn-Moore, F.; Yan, S. D.; Lustbader, J.; Stern, A. R.; Stern, D. M.; Brady, R. L. Recognition of Structurally Diverse Substrates by Type II 3-Hydroxyacyl-CoA Dehydrogenase (HADH II)/Amyloid-β Binding Alcohol Dehydrogenase (ABAD)1. *J. Mol. Biol.* **2000**, *303*, 311–327.

(17) Gangloff, A.; Shi, R.; Nahoum, V.; Lin, S.-X. Pseudo-Symmetry of C19 Steroids, Alternative Binding Orientations, and Multispecificity in Human Estrogenic 17beta-Hydroxysteroid Dehydrogenase. *FASEB J.* **2003**, *17*, 274–276.

Table of Contents graphic.

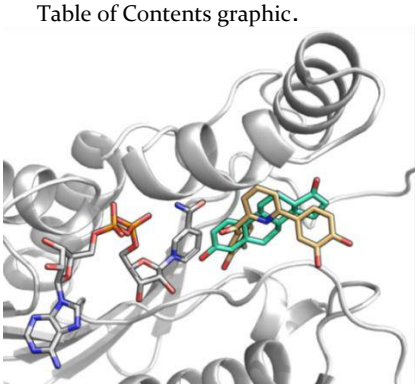

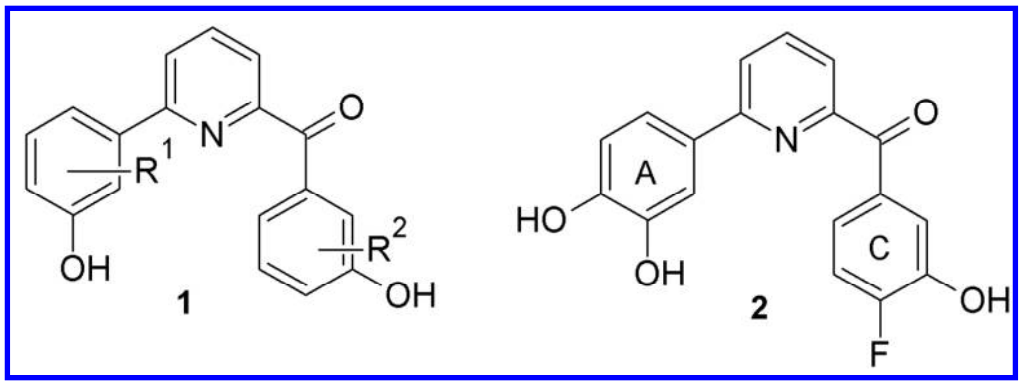

Figure 1. Structure of dihydroxyphenylpyridine methanone scaffold 1 and compound 2

130x47mm (300 x 300 DPI)

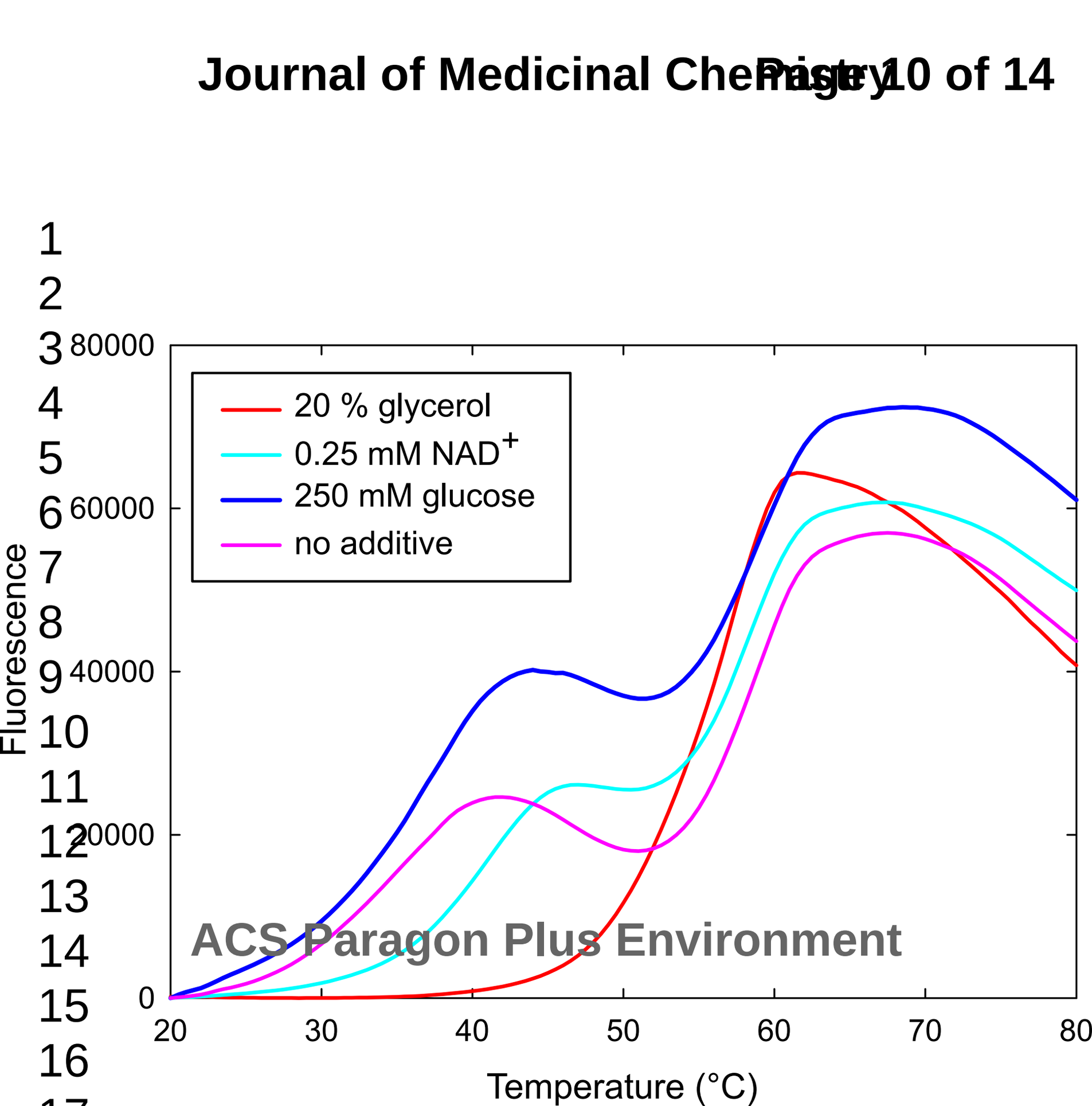
80000
60000
40000
20000
0
Fluorescence
20 % glycerol
0.25 mM NAD+
250 mM glucose
no additive
ACS Paragon Plus Environment
20
30
40
50
60
70
80
Temperature (°C)

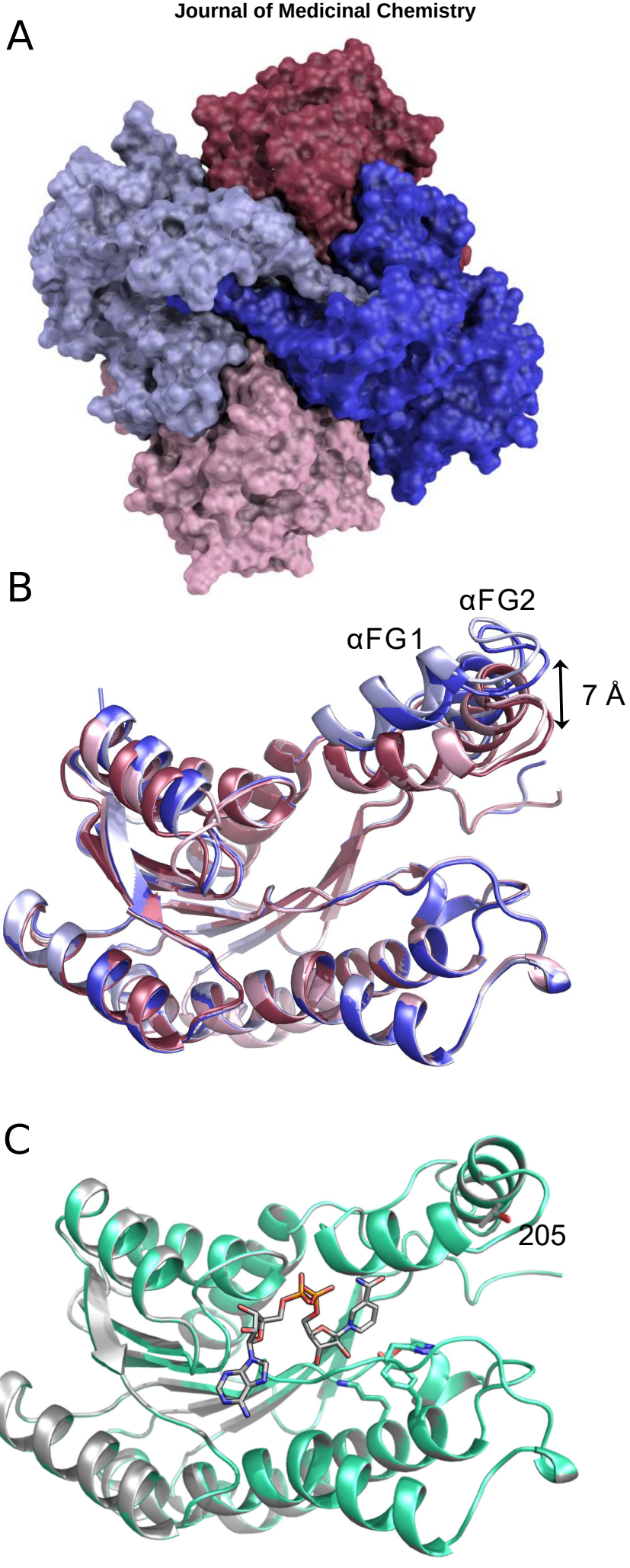
A
B
αFG2
αFG1
7 Å
C
205

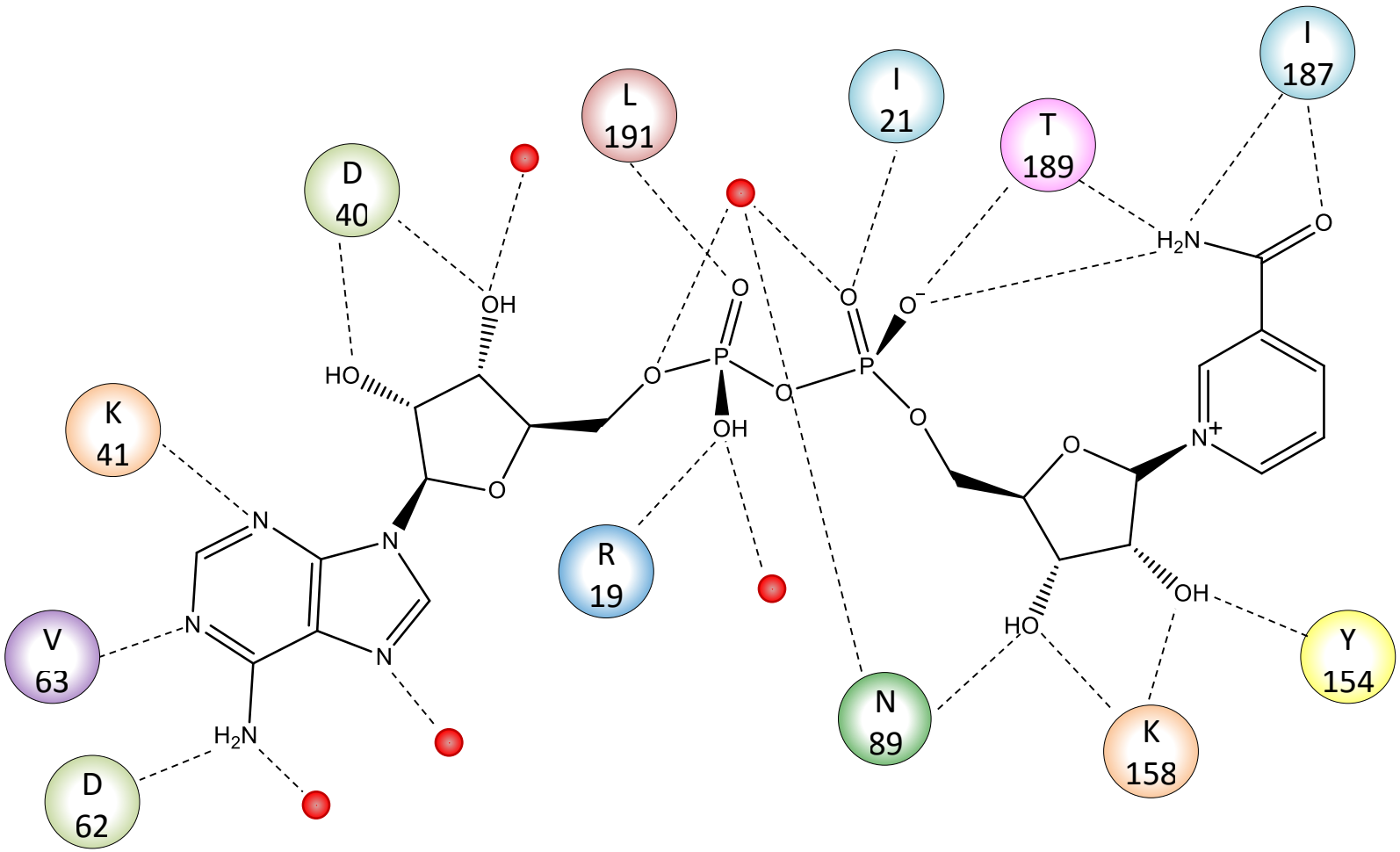
I
187
L
191
I
21
T
189
D
40
K
41
R
19
V
63
D
62
N
89
K
158
Y
154
OH
HO
O
P
N
N+
H2N

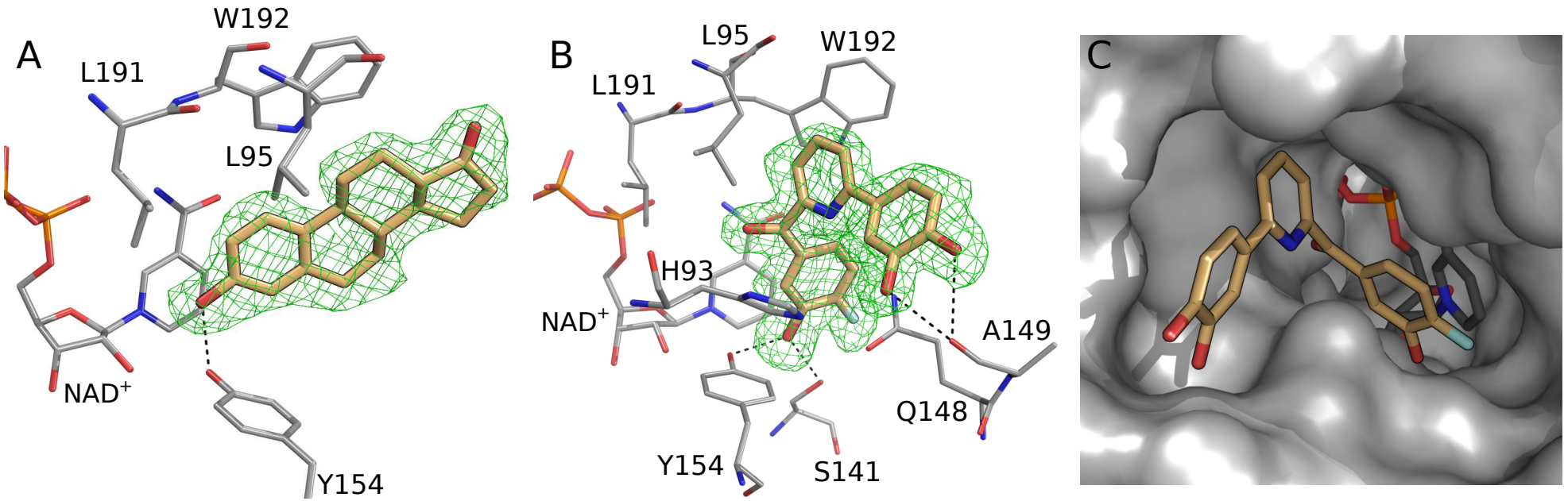
A
W192
L191
L95
NAD+
Y154
B
L95
W192
L191
H93
NAD+
A149
Q148
Y154
S141
C